

m_1 . Our spectra also contain a weak component at the cylinder frequency, F_{cyl} , due to slight misalignment within the Couette system, and the spectral lines are broadened because of poor table speed control. Detailed measurements with improved system alignment and speed control will be made for all of the observed states (m_1, m_2).⁹

In conclusion, we have shown that doubly periodic flow in the Couette system corresponds to two traveling waves that propagate with different speeds. The symmetry arguments of Rand⁴ and Gorman, Swinney, and Rand⁵ suggest that there may be other cylindrically symmetric fluid systems with this feature. In fact, Pfeffer and Fowlis¹⁰ have described an asymmetrical flow state observed in a differentially heated rotating annulus in terms of the superposition of two traveling waves.

Several questions are raised by these results. For example, why does simple superposition appear to generate the observed space-time symmetries? Also, what is the physical significance of two wave speeds? If the flow is locally perturbed, will the effect of the perturbation travel at either or both speeds? These and other questions remain for future investigations.

We thank Jack Swift and Michael Gorman for stimulating discussions. This work is supported by National Science Foundation Grant No. CME79-

09585.

^(a)Permanent address: Department of Physics, University of California, Santa Cruz, Cal. 95060.

^(b)Permanent address: Bell Laboratories, Murray Hill, N.J. 07974.

¹R. C. DiPrima and H. L. Swinney, in *Hydrodynamic Instabilities and the Transition to Turbulence*, edited by H. L. Swinney and J. P. Gollub (Springer, Berlin, 1981), p. 138.

²D. Coles, *J. Fluid Mech.* **21**, 385 (1965).

³M. Gorman and H. L. Swinney, *Phys. Rev. Lett.* **43**, 1871 (1979), and *J. Fluid Mech.* **117**, 123 (1982).

⁴D. Rand, to be published.

⁵M. Gorman, H. L. Swinney, and D. Rand, *Phys. Rev. Lett.* **46**, 992 (1981).

⁶P. R. Fenstermacher, H. L. Swinney, and J. P. Gollub, *J. Fluid Mech.* **94**, 103 (1979).

⁷The relations between the frequencies denoted here F_1 and F_2 and the frequencies denoted f_1 and f_2 in Ref. 3 are $F_1 = f_1$ and $F_2 = f_1 + f_2$.

⁸Equation (2) can be obtained by substituting

$$I(\varphi_1, \varphi_2) = \sum a_p b_q \exp[i(p\varphi_1 + q\varphi_2)]$$

and

$$I(\varphi_1', \varphi_2') = \sum a_p b_q \exp[i(p\varphi_1' + q\varphi_2')]$$

into $D(\delta, \tau; t)$.

⁹C. D. Andereck, R. S. Shaw, L. A. Reith, and H. L. Swinney, to be published.

¹⁰R. L. Pfeffer and W. W. Fowlis, *J. Atmos. Sci.* **25**, 361 (1967).

Observations of Double Layers and Solitary Waves in the Auroral Plasma

M. Temerin, K. Cerny, W. Lotko, and F. S. Mozer

Space Sciences Laboratory, University of California, Berkeley, California 94720

(Received 29 January 1982)

Small-amplitude double layers and solitary waves containing magnetic-field-aligned electric field components have been observed for the first time in the auroral plasma between altitudes of 6000 and 8000 km in association with electron and ion velocity distributions that indicate the presence of electric fields parallel to the magnetic field. The double layers may account for a large portion of the parallel potential drop that accelerates auroral particles.

PACS numbers: 53.35.Fp, 52.35.Mw, 94.30.Gm

Double layers, small localized regions of a single electric field polarity, have been studied analytically,¹ but until now have been observed only in computer simulations² and in laboratory plasmas.³ We report the first observation of small-amplitude double layers in a naturally occurring plasma. These double layers differ from the previously reported electrostatic shocks⁴

in that their electric field is much smaller (typically no greater than 15 mV/m), their electrostatic polarization relative to the magnetic field is predominantly parallel rather than perpendicular, and the duration of an individual double layer is much shorter—typically 2–20 ms rather than 0.1–10 s for the electrostatic shocks. The dominant polarity of the electric field through an

individual double layer points toward the magnetosphere. The localized parallel electric field components and net potential jumps identify these structures as double layers. In contrast, the solitary waves possess the properties of double layers except that they contain no net potential. The solitary waves and double layers are not accompanied by other higher-frequency waves up to the 18-kHz limit of the detector.

S3-3 was a polar-orbiting satellite with an apogee of 8000 km and a perigee of 250 km. It was equipped with three orthogonally oriented pairs of spheres, which made a three-component measurement of the electric field.⁵ The satellite spun in a cartwheel fashion with a period of 18 s, so that one of the two radial pairs of spheres was nearly aligned with the magnetic field every 4.5 s. Each of the two pairs of spheres in the radial direction was separated by 37 m, while the pair in the axial direction was separated by 6 m. During portions of the orbit, electric-field wave data with a temporal resolution of 0.1 ms were telemetered to the ground. Other instruments measured ion and electron fluxes.⁶

The top half of Fig. 1 shows three components of the electric field when one pair of spheres was aligned within 6° of the magnetic field. Examples of double layers and solitary waves are marked. Negative parallel electric fields point out of the ionosphere. The perpendicular components of the electric field show low-frequency turbulence, a common feature of auroral-zone data, and electrostatic ion-cyclotron (EIC) waves at about 140 Hz. Notice that both of these features have little or no parallel electric field component. The bottom portion of Fig. 1 shows three components of the electric field 2 s later, when both radial pairs of spheres were oriented at about 45° with respect to the magnetic field. The data have been transformed into a magnetic-field-aligned coordinate system. The purpose of the bottom half of the figure, in addition to showing another example of the data, is to demonstrate that the observations are not interference features that depend on the antenna orientation.

The double layers and solitary waves shown in Fig. 1 represent only a small portion of the ~ 400 events that were observed in the 45-s interval that coincided with a region of upgoing ion beams and enhanced loss cones in the ~ 0.5 -keV electron distribution. These particle signatures indicate the presence of a potential drop below the satellite of about 0.5 kV.⁷ In addition, enhanced downward fluxes of electrons and a slight local minimum in

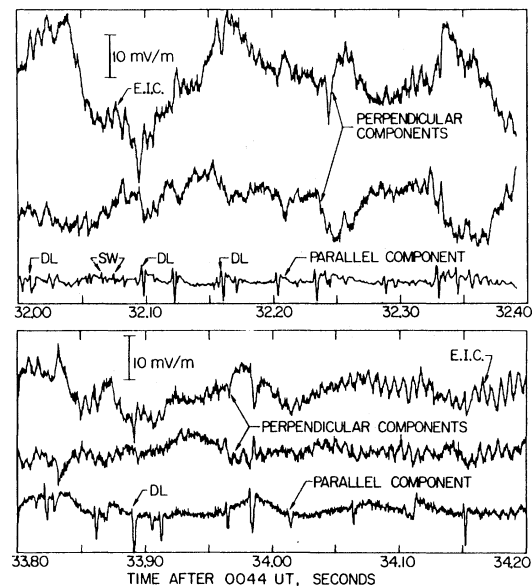


FIG. 1. The two perpendicular and one parallel electric field components shown. Examples of double layers (DL), solitary waves (SW) and electrostatic ion cyclotron (EIC) are marked. These data were acquired on August 11, 1976, at an altitude of 6030 km, an invariant latitude of 74.1° , and a magnetic local time of 15.74 h. The finite parallel component of the low-frequency turbulence (i.e., ~ 10 Hz) in the lower half of the figure is an artifact due to frequency-dependent gain of the detectors at low frequencies.

the electron pitch angle distribution at 90° indicate the presence of a parallel electric field above the satellite.

About 100 min of data during times when the S3-3 satellite was in the auroral zone at altitudes between 2000 and 8000 km have been examined. Six additional groups of interspersed double layers and solitary waves, ranging in number between 10 and 400, were found between 6000 and 8000 km altitude. All were located in regions where upgoing ion beams and electron pitch-angle distributions indicated the presence of parallel electric field both below and above the satellite. The double layers in each group had an irregular recurrence period that, on the average, was approximately 0.1 s. EIC waves occurred in all cases coinciding with or within a few seconds of all double-layer observation. EIC waves are known to be well correlated with observations of upflowing ions.⁸

A major goal of auroral physics is to determine the origin and distribution of the parallel electric fields that accelerate the electrons that produce the visible aurora. The presence of double

layers in regions of parallel electric fields suggests that the net potential through a series of small-amplitude double layers distributed along the magnetic field may account for much of the total potential drop in these regions. In the 45-s interval surrounding the data in Fig. 1, double layers were observed approximately 5% of the time with typical parallel electric fields the order of 10 mV/m. Thus, the average parallel electric field component produced by the double layers was ~ 0.5 mV/m. This electric field, distributed over an altitude range the order of 1000 km, would give a net potential of about 0.5 kV, which would account for the observed particle distribution functions. It should be noted that the 45-s interval corresponded to 0.5° in invariant latitude, which is the scale size over which large-scale parallel electric field acceleration⁹ ("inverted V's") is known to occur, rather than the scale size of individual electrostatic shocks.

To find the parallel potential drop through an individual double layer, it is necessary to know the length of the double layer in the direction parallel to the magnetic field. The 37-m boom length is a lower limit on the length since the opposite-polarity electric fields in any single structure are not separated by an extended region of near-zero electric field. Another estimate may be obtained if the double-layer velocity along the magnetic field is known. In principle, the double-layer velocity relative to the spacecraft can be determined by comparing the onset of the event in two sets of double probes oriented in different directions as illustrated in Fig. 2. The double probe labeled "V34" is extended 9 m further along the magnetic field than is V12, and so it should be the first to detect any pulse coming either up or down the magnetic field. The best estimate for the example in Fig. 2 is that the V34 double probe detects the double layer 0.2 ± 0.3 ms before the V12 double probe, which corresponds to a velocity of ~ 45 km/s and a parallel length of 300 m. Other such estimates give typical time delays that are also zero within the ~ 0.3 -ms uncertainty of the measurements.¹⁰ Therefore, in fact, such estimates can give only a lower limit for the velocity, which is the order of or greater than 50 km/s. For comparison, the velocity of 500-eV H^+ (the typical energy of the ion beam in the regions of the double layers) is 310 km/s. The parallel velocity estimate of ≈ 50 km/s combines with the ~ 4 ms typical duration of an event to give a parallel double-layer scale length of ≈ 200 m. This lower limit on the scale

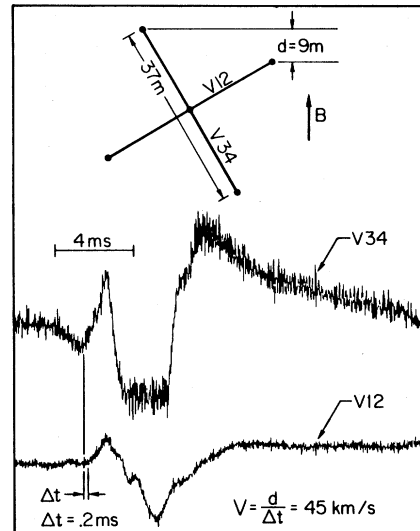


FIG. 2. A comparison of the data from two double sphere electric field detectors oriented with respect to the magnetic field (B) as shown in the top portion of the figure. The flat portions of the data at the extrema of the output of V34 are due to saturation.

length and the observed ~ 10 -mV/m field combine to yield an estimate of more than a few volts for the net potential in a double layer.

While no direct measurements of density and temperature were made simultaneously with observations of double layers, Langmuir probe measurements⁵ from similar regions of space indicate electron densities of $\sim 5 - 10$ cm^{-3} and electron temperatures of $\sim 0.5 - 5$ eV for the cold component. In addition, particle measurements show a hot "plasma sheet" electron component with a density of 1 cm^{-3} and a temperature of 0.5 keV. Since the Debye length depends mostly on the cold component, the corresponding Debye length (λ_D) is in the range of 5 m. Thus, the double-layer thickness parallel to the magnetic field is the order of or greater than $40\lambda_D$ and the average double-layer separation is the order of or greater than $800\lambda_D$. The scale length perpendicular to the magnetic field is more difficult to estimate. Planar structures should produce similar signals in all detectors, except for differences in polarity and magnitude. This is often not the case, as can be seen in a few examples in Fig. 1 indicating that the perpendicular scale length of an individual double layer can be comparable to the parallel scale length. Such transverse structure may indicate that the double layers and solitary waves propagate obliquely, are modulationally unstable,¹¹ or are intrinsically

nonplanar electrostatic perturbations. In any case, the important feature of the double layers is their average parallel electric field and potential drop.

The data presented here are, in many ways, similar to the results of computer simulations wherein current-driven double layers form with a longitudinal scale of ~ 50 Debye lengths, are separated by about ~ 1000 Debye lengths, have potential drops the order of or less than the electron thermal energy, are preceded by negative potential spikes with a scale length the order of 10 Debye lengths, and emit ion-acoustic solitons as they decay.² The negative potential spike is thought to play a crucial role in the formation of the double layer by reflecting a portion of the current-carrying electrons, thus establishing a charge imbalance.^{2, 12} The observed double layers also often have this oppositely directed electric field which precedes the larger double-layer electric field pulse and are also frequently associated with solitary waves. Exact comparisons between simulations and data are difficult because the wave propagation direction relative to the spacecraft cannot be unambiguously determined from our single-spacecraft measurement. This ambiguity allows two interpretations of the data, as indicated in Fig. 3. The first wave form, (1), is preceded by a positive-potential compressive pulse as it propagates toward the ionosphere. The second wave form, (2), is preceded by a negative-potential rarefactive pulse propagating toward the magnetosphere. The latter structure resembles the current-driven double layers seen in simulations. A recent study¹³ of ion-acoustic soliton dynamics in collisionless auroral plasma indicates that downward propagating compressive modes are damped by ion reflection dissipation, whereas upward propagating rarefactive modes can be resonantly amplified by coupling to the field-aligned electron current. This analysis favors wave form (2) as the

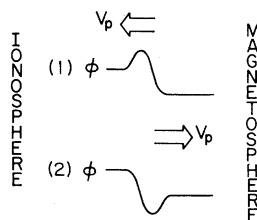


FIG. 3. Two possible potential structures for the double layer which are consistent with the data.

correct interpretation. Also the upward-directed, supersonic ion beams associated with these events have the effect of Doppler shifting the wave propagation velocity in the beam direction.¹³

Small-amplitude double layers may explain the fine structure of auroral kilometric radiation. The fine structure consists of many rising and falling tones; this has been interpreted as the motion of the source region down and up the magnetic field line at velocities between 3 and 300 km/s. The width of the tone indicates a source-region size of less than 50 km. It has been hypothesized that the fine structure is due to moving double layers.¹⁴ Although we are not capable of measuring kilometric radiation, it seems reasonable to suppose that we have observed these double layers. Some caution is required, however, since the kilometric source region is observed to move both up and down the magnetic field line, while the observations reported here are all in upward ion beam regions, suggesting that these structures may be moving upward.

We have shown that small-amplitude double layers and solitary waves exist in the collisionless auroral plasma in association with regions of parallel electric fields. The double layers may account for a large portion of the total potential on auroral field lines and may be responsible for the fine structure of auroral kilometric radiation. The formation of these nonlinear waves in the auroral plasma remains an outstanding problem.

This research was supported in part by the U. S. Office of Naval Research under Contract No. N00014-75-C-2094 and in part by the National Science Foundation under Grant No. ATM-8103347.

¹L. P. Block, *Cosm. Electrodyn.* **3**, 349 (1977); J. R. Kan and L. C. Lee, *Geophys. Res. Lett.* **7**, 429 (1980); S. Torvén, *Phys. Rev. Lett.* **47**, 1053 (1981).

²T. Sato and H. Okuda, *J. Geophys. Res.* **86**, 3357 (1981); M. K. Hudson and D. W. Potter, in *Physics of Auroral Arc Formation*, edited by S. I. Akasofu and J. R. Kan (American Geophysical Union, Washington, D.C., 1981), p. 260; J. M. Kindel, C. Barnes, and D. W. Forslund, *ibid.*, p. 296.

³B. H. Quon and A. Y. Wong, *Phys. Rev. Lett.* **37**, 1393 (1976); S. Torvén and D. Anderson, *J. Phys. D* **12**, 717 (1979); P. Coakley, L. Johnson, and N. Hershkowitz, *Phys. Lett.* **70A**, 425 (1979); P. Leung, A. Y. Wong, and B. H. Quon, *Phys. Fluids* **23**, 992 (1980); Ch. Holtenstein, M. Gogot, and E. S. Weibel, *Phys. Rev. Lett.* **45**, 2110 (1980); N. Hershkowitz, G. L. Payne, C. Chun,

and J. R. DeKock, *Plasma Phys.* **23**, 903 (1981).

⁴F. S. Mozer *et al.*, *Phys. Rev. Lett.* **38**, 292 (1977);
F. S. Mozer *et al.*, *Space Sci. Rev.* **27**, 155 (1980).

⁵F. S. Mozer *et al.*, *J. Geophys. Res.* **84**, 5875 (1979).

⁶P. F. Mizera and J. F. Fennel, *Geophys. Res. Lett.* **4**, 311 (1977); E. G. Shelley, R. D. Sharp, and R. G. Johnson, *Geophys. Res. Lett.* **3**, 654 (1976); R. D. Sharp, R. G. Johnson, and E. G. Shelley, *J. Geophys. Res.* **82**, 3324 (1977).

⁷R. D. Croley, Jr., P. F. Mizera, and J. F. Fennel, *J. Geophys. Res.* **83**, 2761 (1978).

⁸P. M. Kintner *et al.*, *J. Geophys. Res.* **84**, 7201 (1979). See also M. A. Temerin, M. Woldorff, and F. S. Mozer, *Phys. Rev. Lett.* **43**, 1941 (1979); P. M. Kintner, *Geophys. Res. Lett.* **7**, 585 (1980), for other examples of ion-associated waves on auroral field lines. Space limitations prevent discussion of other solitary waves not associated with double layers seen in conjunction with steepened electrostatic ion-cyclotron waves.

⁹L. A. Frank and K. L. Ackerson, *J. Geophys. Res.* **76**, 3612 (1971).

¹⁰The uncertainty in the velocity estimate is due in part to the different gains and telemetry noise levels associated with the two double probes, which make it difficult to key on similar features in the data.

¹¹E. W. Laedke and K. W. Spatschek, *Phys. Rev. Lett.* **47**, 719 (1981).

¹²A. Hasagawa and T. Sato, *Bull. Am. Phys. Soc.* **25**, 844 (1980).

¹³W. Lotko, Ph.D. thesis, University of California, Los Angeles, 1981 (unpublished).

¹⁴D. A. Gurnett and R. R. Anderson, in *Physics of Auroral Arc Formation*, edited by S. I. Akasofu and J. R. Kan (American Geophysical Union, Washington, D.C., 1981), p. 341. Also see J. L. Green, D. A. Gurnett, and R. A. Hoffman, *J. Geophys. Res.* **84**, 5211 (1979); W. Calvert, *Geophys. Res. Lett.* **8**, 919 (1981), for other relevant features of auroral kilometeric radiation.

Stimulated Raman Scattering from uv-Laser-Produced Plasmas

K. Tanaka, L. M. Goldman,^(a) W. Seka, M. C. Richardson, J. M. Soures, and E. A. Williams
Laboratory for Laser Energetics, University of Rochester, Rochester, New York 14627
(Received 14 December 1981)

Time-integrated, spectrally resolved measurements between 400 and 750 nm have been made of light backscattered from plasmas produced by 450-psec pulses from a 351-nm laser at 10^{13} to 10^{15} W/cm². Threshold and saturation behavior for the two-plasmon decay and the absolute and convective Raman instabilities have been observed. The scattered light spectra suggest the presence of a steepened density profile at the quarter critical density.

PACS numbers: 52.25.Ps, 52.35.-g, 52.50.Jm, 52.70.Kz

Parametric processes in laser-produced plasmas can be sources of energetic electrons which, through their long mean free paths, may preheat the target core in laser fusion experiments and thus influence the hydrodynamics significantly.¹ Among the parametric processes, stimulated Raman scattering (SRS) and the two-plasmon ($2\omega_p$) decay instability may be efficient generators of hot electrons,² especially in the extensive underdense plasmas expected for inertial-confinement fusion targets. Observations of SRS from plasmas produced by 1064- and 532-nm lasers have recently been reported in the literature.³ The existence of the $2\omega_p$ instability has variously been inferred from $\frac{3}{2}\omega_0$ measurements⁴ and from direct plasma wave observations in CO₂-laser-produced plasmas by Baldis, Samson, and Corkum.⁵

In this Letter, we report backscattering measurements from plasmas produced by 351-nm

laser light which demonstrate (as a function of intensity) clear thresholds and low-level saturation for the $2\omega_p$ instability as well as for the absolute (SRS-A) and convective (SRS-C) Raman instabilities. Broad continuum spectra between 400 and 700 nm were observed for the SRS-C instability. The relatively small frequency change ($\Delta\omega$) associated with the low-wavelength limit of these spectra indicates that SRS is operative in plasma densities as low as $0.05n_c$ (n_c is the critical density for 351-nm radiation). The measurements do show the expected lower threshold for the $2\omega_p$ instability relative to the SRS-A instability as predicted by theory. However, the SRS-C is found to have approximately the same threshold as the SRS-A instability, instead of the considerably higher threshold expected if both instabilities operate in plasmas with comparable scale lengths.

The experiments described here were performed